

The time-of-propagation counter for Belle II

K. Nishimura on behalf of the Belle II Particle Identification Group

Department of Physics and Astronomy, University of Hawaii, 2505 Correa Road, Honolulu, HI 96822, USA

Abstract

The Belle II detector operating at the future upgrade to the KEKB accelerator will perform high-statistics precision investigations into the flavor sector of the Standard Model. As charged hadron identification is a vital element of the experiment's success, the time-of-propagation (TOP) counter has been chosen as the primary particle identification device in the barrel region of Belle II. The TOP counter is a compact variant of the detection of internally reflected Cherenkov light (DIRC) technique and relies heavily on exquisite single photon timing resolution with micro-channel plate photomultiplier tubes. We discuss the general principles of TOP operation and optimization of the Belle II TOP configuration, which is expected to provide 4 sigma or better separation of kaons and pions up to momenta of approximately 4 GeV/c.

Keywords: particle identification, detection of internally reflected Cherenkov light (DIRC), time-of-propagation

1. Introduction

The Belle [1] and BaBar [2] experiments at the KEKB and PEP-II B factories have collected a combined integrated luminosity of over 1.5 ab^{-1} . This wealth of data has resulted in a number of precision measurements, including confirmation of the Kobayashi-Maskawa mechanism of CP violation. Charged particle identification (PID) systems have played a significant role in both experiments by providing discrimination between K^\pm and π^\pm , and hence enhancing efficiencies for detecting rare B decays as well as improving the flavor tagging necessary for extracting time-dependent CP asymmetries. In order to further probe the Standard Model and search for new physics, detectors at the next generation super B factories will need increasingly precise PID devices that can accommodate larger background rates due to significantly higher luminosities.

To deal with these challenges, the Belle II detector will replace the existing barrel region time-of-flight counter and threshold aerogel Cherenkov counter with a time-of-propagation (TOP) counter. The TOP technique is a compact variant of the detection of internally reflected Cherenkov light (DIRC) method [3], wherein Cherenkov photons emitted as a charged particle passes through a ra-

diator material, such as a fused-silica bar, are carried by total internal reflection to the bar's end and detected on an imaging plane. In contrast to the BaBar DIRC, which uses two dimensional imaging on a $\sim \text{m}^2$ image plane along with $\sim \text{ns}$ timing to reject backgrounds, the TOP counter will use a compact $\sim 100 \text{ cm}^2$ image plane near the bar end, and further use micro-channel plate photomultiplier tubes (MCP-PMTs) with timing precision of ~ 40 ps to further distinguish particle types. We describe the proposed geometry of the Belle II TOP detector, including the choice of MCP-PMTs and read-out electronics, as well as simulated performance for K/π separation.

2. Principle of Operation

The basic TOP counter schematic is shown in Fig. 1 [4]. A charged particle of a given momentum, which is measured by the tracking subdetectors, passes through a radiator material, emitting Cherenkov photons in a cone with opening angle, θ_C , determined by the particle velocity, β . Thus, the characteristic cone will be unique for particles of different mass. A fraction of the photons are transported down the bar via total internal reflection, and the characteristic pattern is measured in

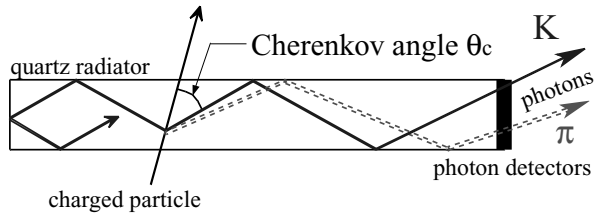


Figure 1: A schematic side-view of a TOP counter.

time and one or more spatial dimensions by PMTs mounted directly to the bar end. The time-of-propagation of each photon from its emission point to the detector plane is correlated with θ_C . Additionally, photon arrival times are typically measured relative to the time of the collider event, so photons are further separated in time by the time-of-flight of the species of charged particle.

The simplest TOP counter reads out only information in one spatial direction and in time. A typical hit pattern for this type of detector is shown in Fig. 2. Arrival time differences between photons from kaons and pions for any given channel differ by order ~ 100 ps at 2 GeV/c, and less at higher momenta. For best performance, the timing resolution of any TOP photodetector must be significantly smaller than this separation. The overall time resolution is limited by chromatic dispersion in the radiator material. To mitigate this effect, a filter material can be placed in front of the MCP-PMTs, limiting detected wavelengths to those where chromatic effects are less pronounced. A focusing mirror can also be added to one end of the radiator bar [5]. Along with finer segmentation in the other spatial direction, this allows some photons of different colors, and thus slightly different θ_C , to focus on different photodetector channels. The focusing element can also remove ambiguities in the photon emission point due to the finite bar thickness. At the cost of some compactness, the image plane can be expanded beyond the end of the bar for improved spatial resolution [6].

3. Detector Configuration

Two designs have been studied for use in the Belle II detector, each shown schematically in Fig. 3. In both cases the design consists of a barrel of 16 TOP modules. The radiator cross section is approximately 440 mm wide by 20 mm thick. Because there is no strong optimum in performance

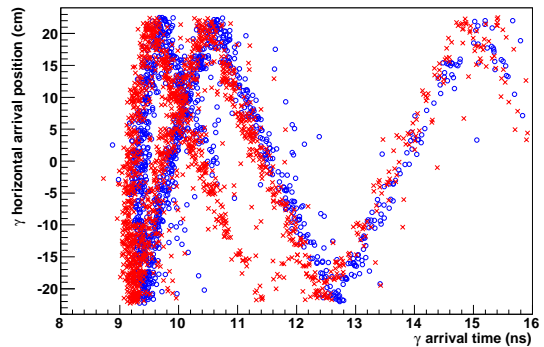


Figure 2: A typical hit pattern in the horizontal bar dimension versus arrival time for a simple TOP counter, consisting of an ensemble of 100 events each for incident pions (red crosses) and kaons (blue circles).

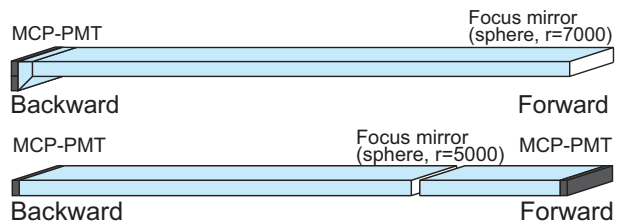


Figure 3: Conceptual sketches of the 1-bar and 2-bar TOP baseline designs.

for the width of the bar, the chosen width represents a reasonable compromise between manufacturing cost, mechanical stability, and overall acceptance. The thickness represents a trade-off between increased light yield and a larger mass in front of the calorimeter.

The 1-bar design, also referred to as an imaging TOP (iTOP), employs a radiator of length ~ 2.75 m, with a spherical mirror placed on the forward end and an expansion prism on the backward end, resulting in an image plane approximately twice the size of the bar cross-section. This creates a larger image plane and thus clarifies the ring image and improves the wavelength separation. In the 2-bar design, two radiators are used. The “long” radiator in the backward direction is reduced in length relative to the 1-bar design, reducing the effect of chromatic dispersion. As in the 1-bar design, this radiator utilizes a spherical mirror in the forward direction. The two bars are read out directly at the ends, resulting in two separate detector planes, each of size equivalent to the bar cross section. In both designs, a wavelength filter of $\lambda \gtrsim 400$ nm is

introduced in front of the PMTs to further reduce chromatic effects.

The full detector consists of a barrel of 16 modules. Due to gaps between the sides of each bar to accommodate the expansion volume and/or support structures, the azimuthal acceptance for charged tracks is $\sim 95\%$.

4. Photodetectors and Readout Electronics

The baseline MCP-PMT for the Belle II TOP is the Hamamatsu SL-10 [7], shown in Fig. 4. The SL-10 has a pore size of $10\ \mu\text{m}$ and a single photon timing resolution of $\sim 40\ \text{ps}$. An aluminum protection layer on the second of two MCPs protects against ion feedback and prevents premature aging of the photocathode. A 4×4 anode configuration will be used, resulting in a total of 512 channels per TOP module, or ~ 8200 channels for the entire barrel. Existing prototypes utilize a multi-alkali photocathode, but efforts are currently underway to switch to a super bi-alkali photocathode and increase overall quantum efficiency.

The large number of readout channels and space constraints of the detector necessitate compact front-end electronics. To accommodate this need while maintaining high precision timing, the Belle II TOP counter will utilize a waveform sampling application specific integrated circuit (ASIC) for readout of the MCP-PMTs. Timing precision of $\leq 30\ \text{ps}$ with an analog bandwidth of approximately $1\ \text{GHz}$ has been obtained with the existing LABRADOR3 ASIC [8]. Belle II will utilize a Buffered LABRADOR (BLAB) ASIC, which adds front-end amplification for detection of single photo-electron signals and significantly deeper sampling to accommodate the expected trigger latencies of up to $5\ \mu\text{s}$.

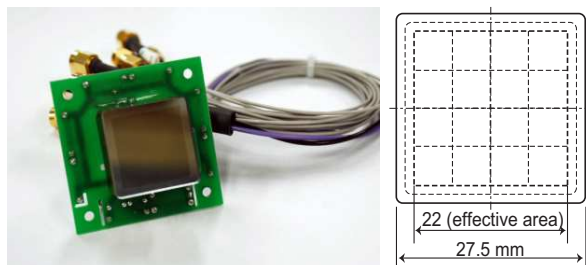


Figure 4: SL-10 prototype MCP-PMT photograph (left) and anode structure diagram (right).

Two generations of BLAB ASICs have been tested with the fDIRC prototype. The first generation BLAB1 [9] was utilized for 16 channels of PMT readout in a beam test of the focusing DIRC (fDIRC) prototype [10], where it obtained timing resolutions competitive with conventional constant fraction discrimination techniques. The second generation BLAB2 has been used to instrument the same fDIRC prototype at a cosmic ray test stand [11]. In this case a compact, integrated photodetector readout was developed and implemented, allowing readout of approximately 450 channels. The TOP detector will utilize the BLAB3 ASIC, with specifications listed in Table 1.

Table 1: Required specifications for the BLAB3 readout ASIC.

Parameter	Value
Channels/BLAB3	8
Analog bandwidth	$\geq 500\ \text{MHz}$
Sampling speed	4 Giga-samples/second
Samples/channel	32768
Amplifier gain	60 relative to $50\ \Omega$ signal
Trigger channels	8
Effective resolution	≈ 9 bits
Sample convert window	64 samples ($\approx 16\ \text{ns}$)
Readout granularity	1 sample, random access
Readout time for n samples	$1 + n \cdot 0.02\ \mu\text{s}$
Sustained level 1 trigger rate	30 kHz

Information from the front-end will be transferred to the rest of the Belle II data acquisition and trigger systems via fiberoptic links. Back-end electronics provide online waveform processing, performing feature extraction on full waveforms and reducing the large raw data volume to a manageable size.

5. Expected Performance

Monte Carlo simulations have been performed to estimate the K/π separation performance of the proposed TOP geometries. Three independent simulations have been performed. The first utilizes GEANT3 [12] to generate the initial charged tracks as well as simulate electromagnetic and hadronic interactions; a stand-alone routine is then used to track optical photons to their final detection at the image plane. The second uses Geant4 [13] to initiate the primary track, simulate electromagnetic interactions, and perform optical propagation to

the detector plane. The last utilizes stand-alone code to simulate Cherenkov emission in the bar and track photons to the detector plane; in this set of simulations no secondary interactions are included. All three simulations include measured distributions for the time and spectral response of the MCP-PMTs. Beam tests have been performed [14] and validate the simulation results.

To determine expected efficiencies and fake rates for K/π discrimination, the detected photons for each track are tested against probability distribution functions (PDFs) for each particle hypothesis ($\mathcal{P}^K(x, t)$ and $\mathcal{P}^\pi(x, t)$). From these PDFs, a likelihood is determined for a simulated primary charged particle at a given incident angle and impact position. For the Geant based simulations, PDF values are obtained from an ensemble of a large number of simulated events. For the fully stand-alone code, an analytical technique is used to calculate PDF values [15].

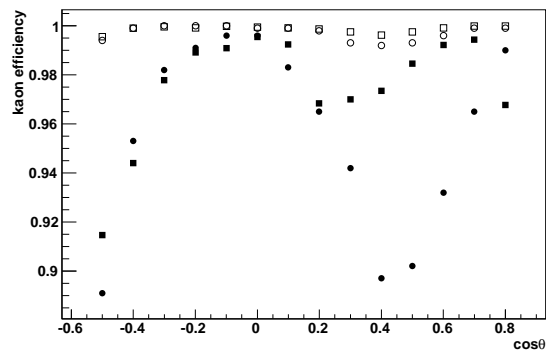


Figure 5: Geant4-based simulated kaon efficiency as a function of cosine of track polar angle for the 1-bar (circles) and 2-bar (squares) configurations at track momenta of 2 GeV/c (open) and 3 GeV/c (filled).

Example distributions of kaon efficiency for the Geant4 simulations are shown in Fig. 5. The three simulations show reasonable agreement, particularly in terms of reproducing similar features as a function of track impact angle. A dip in performance is observed for the 1-bar design at a polar angle of $\sim 60^\circ$, and is attributed to chromatic dispersion due to the increased propagation length of the photons. The same feature is seen in the 2-bar design around $\sim 70^\circ$, but is less pronounced due to the shorter bar length. The two bar design also shows a noticeable drop in performance in the very forward direction. In this region, the short forward bar serves primarily as a time-of-

flight counter, since the characteristic ring images do not separate significantly temporally or spatially before detection. Despite these differences between configurations, the expected overall differences for representative physics modes are mild. For example, Table 2 shows performance for the decay $B \rightarrow \rho\gamma, \rho \rightarrow \pi\pi$, which suffers from a large background from $B \rightarrow K^*\gamma, K^* \rightarrow K\pi$. Differences in pion efficiencies and kaon misidentification rates for the two TOP designs are less than a percent in all simulations. Efforts are continuing to improve simulations, add all appropriate effects, and test the analytical reconstruction method on GEANT3 and Geant4 simulation data.

Table 2: Simulated pion efficiencies, ϵ_π , and kaon misidentification rates, f_K , for the decay $B \rightarrow \rho\gamma$ with a background of $B \rightarrow K^*\gamma$, under nominal expected conditions.

	ϵ_π (%)		f_K (%)	
	1-bar	2-bar	1-bar	2-bar
GEANT3	98.6	98.9	0.9	1.0
Geant4	99.9	99.9	0.4	0.2
Stand-alone	99.1	99.6	0.4	0.4

These simulations have been used to study various effects and uncertainties. Small or negligible effects are observed for possible mirror misalignment and beam background rates. More significant effects are observed due to uncertainties from the tracking systems and jitter in the measurement of the event start time, t_0 . The 1-bar design is more sensitive to the former and the 2-bar design to the latter, though the two designs otherwise perform comparably. While the expected tracking uncertainties are relatively well understood, the final expected t_0 jitter is much less clear. For this reason, as well as because of the larger acceptance in the forward direction and the simplicity of a single detector plane, the 1-bar iTOP has been chosen as the baseline design.

6. Conclusion

Belle II will utilize a TOP counter for PID in the barrel region, as its compact design means it can be integrated into the limited space available in the Belle II environment. Two designs have been studied: a 2-bar configuration with two readout planes and a 1-bar configuration with a single, larger image plane. Both configurations utilize the Hamamatsu SL-10 MCP-PMT as the photodetector, as

this device meets the extreme timing requirements required for the TOP technique. Electronics based on a custom waveform sampling ASIC, the BLAB3, will perform front-end readout of the photodetectors and interface to the back-end data and trigger system. Simulation of both configurations indicates tradeoffs between the two geometries for various event uncertainties and impact positions. In both cases, performance is expected to surpass the existing Belle PID systems, allowing 4 sigma separation of kaons and pions up to momenta of 4 GeV/c.

References

- [1] A. Abashian *et al.* (Belle Collaboration), Nucl. Instrum. Meth. A **479**, 117 (2002).
- [2] B. Aubert *et al.* (BaBar Collaboration), Nucl. Instrum. Meth. A **479**, 1 (2002).
- [3] I. Adam, *et al.* (BaBar-DIRC Collaboration), Nucl. Instrum. Meth. A **538**, 281 (2005).
- [4] K. Inami, Nucl. Instrum. Meth. A **595**, 96 (2008).
- [5] B. Ratcliff, Nucl. Instrum. Meth. A **502**, 211 (2003).
- [6] K. Nishimura, *et al.*, Nucl. Instrum. Meth. A, DOI: 10.1016/j.nima.2010.02.227.
- [7] K. Inami, *et al.*, Nucl. Instrum. Meth. A **592**, 247 (2008).
- [8] G. Varner, *et al.*, Nucl. Instrum. Meth. A **583**, 447 (2007).
- [9] L. Ruckman *et al.*, Nucl. Instrum. Meth. A **591**, 534 (2008).
- [10] J. Benitez *et al.*, Nucl. Instrum. Meth. A **595**, 104 (2008).
- [11] L. Ruckman *et al.*, Nucl. Instrum. Meth. A, DOI: 10.1016/j.nima.2010.02.229.
- [12] R. Brun *et al.*, GEANT 3.21, CERN Report Number DD/EE/84-1 (1984).
- [13] S. Agostinelli *et al.*, Nucl. Instrum. Meth. A **506**, 250 (2003).
- [14] K. Inami, Journal Intr. **5** P03006 (2010).
- [15] M. Staric *et al.*, Nucl. Instrum. Meth. A **595**, 252 (2008).